Catalysis Science & Technology

PAPER

View Article Online
View Journal | View Issue

Cite this: *Catal. Sci. Technol.*, 2015, 5, 2290

DRIFTS study of a Ce–W mixed oxide catalyst for the selective catalytic reduction of NO_x with NH_3

Kuo Liu, Fudong Liu,† Lijuan Xie, Wenpo Shan‡ and Hong He*

Received 26th November 2014,
Accepted 17th January 2015

DOI: 10.1039/c4cy01550a

www.rsc.org/catalysis

A systematic study has been conducted on the reactivity of the selective catalytic reduction of NO_x with NH_3 (NH_3-SCR) in a wide range of NO/NO_2 feed ratios (from 0 : 1 to 1 : 0) over a $CeWO_x$ catalyst prepared by a homogeneous precipitation method. By using *in situ* diffuse reflectance infrared Fourier transform spectroscopy (*in situ* DRIFTS), the roles of NO and NO_2 at low temperatures during the fast SCR reaction have been revealed. NO_2 adsorption results in the formation of surface nitrates, which participate in the NH_3-SCR reaction through two pathways: one path where the nitrates react with NH_3 to form ammonium nitrate (NH_4NO_3), then NO reduces NH_4NO_3 below its melting point to form N_2 (the NH_4NO_3 path); the other path where the surface nitrates are reduced by NO to form active nitrite species that further react with NH_3 to produce N_2 (the nitrate path). "The NH_4NO_3 path" and "the nitrate path" contributed simultaneously to the standard and the fast SCR reaction at low temperatures. Both the surface nitrates and NO in the gas phase were suggested to be necessary for the excellent performance of the fast SCR reaction over the $CeWO_x$ catalyst.

1. Introduction

NO_x, a major source of air pollution, causes photochemical smog and acid rain, which are detrimental to human health. NO_x mainly comes from industrial combustion of fossil fuels and automobile exhaust gas, and NO_x removal from diesel engine exhaust remains a challenge in environmental catalysis.[1,2] The selective catalytic reduction of NO_x with NH_3 (NH_3-SCR) is one of the most effective technologies for NO_x removal from diesel engines.[3] The catalysts for NH_3-SCR can be divided into the following groups, V-based oxide catalysts, Cu or Fe zeolite catalysts, and vanadium-free oxide catalysts. Among these catalysts, the non-toxic vanadium-free oxide catalysts, such as $FeTiO_x$,[4–6] WO_3/CeO_2–ZrO_2,[7] and CeO_x–MnO_x/TiO_2,[8] show good NH_3-SCR performance and H_2O/SO_2 durability over a wide temperature range from 200 to 500 °C. CeO_2 has long been applied as a promoter and carrier for low temperature NH_3-SCR catalysts.[9–11]The use of cerium oxide as a main catalyst for the NH_3-SCR reaction was first reported by Xu *et al.*,[12] and then many other researchers developed Ce-based catalysts applicable for the NH_3-SCR process, *e.g.* CeO_2/Al_2O_3,[13] CeO_2/TiO_2,[14–16] Ce–W–Ti mixed oxides,[17–19] Ce–W mixed oxides,[20–23] and CeO_2–MoO_3/TiO_2.[24] It should be noted that $CeTiO_x$,[15,16] $CeWO_x$,[20] and $CeWTiO_x$ (ref. 19) could eliminate NO completely over a wide temperature range of 250–425 °C, even under a rather high gas hourly space velocity (GHSV) of 500 000 h^{-1}. The prominent performance under high GHSV of the Ce-based catalysts made it worthwhile to further investigate the NH_3-SCR mechanism in detail.

The mechanism of NH_3-SCR over different types of catalysts has been studied by many researchers. Some researchers reported that the NH_3-SCR reaction followed the Langmuir–Hinshelwood (L–H) mechanism at low temperatures (≤200 °C), whereas the Eley–Rideal (E–R) mechanism might take place at high temperatures (>200 °C), *e.g.* on $FeTiO_x$ (ref. 25) or CeO_2/TiO_2.[18] The reaction might also proceed through the E–R mechanism over the whole temperature range, such as on $CeWTiO_2$ catalysts.[18] In other studies, both E–R and L–H mechanisms took place over the whole temperature range simultaneously, such as on $CeWO_x$ catalysts.[21] However, in these reports, the authors mainly focused on the reaction between NO, O_2, and NH_3. It is widely accepted that the oxidation of NO to NO_2 is an important step in the NH_3-SCR reaction. Long and Yang[26] reported that the higher activity of NO oxidation to NO_2 on Fe-ZSM-5 led to improved SCR performance. Similarly, Fe–Mn/TiO_2 showed higher SCR activity than Mn/TiO_2 due to the higher rate of NO oxidation to NO_2.[27] In our previous studies, NO_2 production by NO oxidation was also suggested to be responsible for

State Key Joint Laboratory of Environment Simulation and Pollution Control, Research Center for Eco-Environmental Sciences, Chinese Academy of Sciences, 18 Shuangqing Road, Haidian District, Beijing 100085, China.
E-mail: honghe@rcees.ac.cn; Fax: +86 10 62849123; Tel: +86 10 62849123
† Present address: Materials Sciences Division, Lawrence Berkeley National Laboratory, Berkeley 94720, California, United States.
‡ Present address: School of Environmental and Biological Engineering, Nanjing University of Science and Technology, Nanjing 210094, China.

the promoted SCR activity on $CeTiO_x$ (ref. 15) or on $CeWTiO_x$ at temperatures below 300 °C.[19] The formation of NO_2 might facilitate the fast SCR reaction, resulting in higher SCR activity. Therefore, NO_2 has a great effect on the reaction between NO, O_2, and NH_3. However, to the best of our knowledge, no publications have ever reported the effect of NO/NO_2 feed ratios on the NO_x conversion systematically over the $CeWO_x$ catalyst.

The promotional role of NO_2 in the SCR reaction over V_2O_5–WO_3/TiO_2 and zeolite-based catalysts has been intensively investigated in the last decade. Koebel *et al.*[28] suggested that NO_2 accelerated the SCR reaction over V_2O_5–WO_3/TiO_2 by reoxidizing the V sites. Yeom *et al.*[29] suggested that N_2O_3 formed by equimolar NO/NO_2 reacted with water and NH_3 to produce ammonium nitrite over the BaNa-Y catalyst, which is an unstable species above 100 °C. Others suggested that the fast SCR reaction at low temperatures involved the reduction of nitric acid, surface nitrates and/or ammonium nitrate (NH_4NO_3) by NO.[30–35] At present, it is still a controversial issue how the presence of NO_2 in the feed mixture promotes NO_x elimination. By comparing the mechanisms of standard SCR and fast SCR in the meantime, one can gain a clear view of the NH_3-SCR mechanism, which is helpful to guide the practical application of the studied catalysts. So far, unfortunately, a detailed study of the mechanism of the fast SCR reaction over Ce-based catalysts is still lacking.

In the present study, the SCR reaction has been studied over a wide range of NO/NO_2 feed ratios from 0 : 1 to 1 : 0. The mechanism of the fast SCR reaction over $CeWO_x$ in the low temperature range was investigated by *in situ* DRIFTS. The roles of NO and NO_2 in the SCR reaction have been revealed comprehensively, and for the first time, the reactions between NO and NH_4NO_3 or the surface nitrates have been studied systematically on the $CeWO_x$ catalyst at low temperatures.

2. Experiments

2.1 Catalyst synthesis and activity test

The Ce–W mixed oxide catalyst, with a Ce/W molar ratio of 1 : 1, was prepared by a homogeneous precipitation method, as described in the previous report.[20] Briefly, cerium nitrate ($Ce(NO_3)_3{\cdot}6H_2O$) was first added into a mixed solution containing ammonium tungstate ($(NH_4)_{10}W_{12}O_{41}$) and an equal weight of oxalic acid ($H_2C_2O_4{\cdot}2H_2O$), and then an aqueous urea solution was added into the mixture, with a urea/(Ce + W) molar ratio of 10 : 1. The mixed solution was then heated at 90 °C for 12 h under vigorous stirring. After filtration and washing, the sample was dried at 100 °C overnight and successively calcined at 500 °C for 5 h. The obtained catalyst was denoted as $CeWO_x$. The powder $CeWO_x$ catalyst was pressed and crushed to 40–60 mesh before the activity tests.

The SCR activity tests were performed in a fixed-bed quartz flow reactor at atmospheric pressure using 100 mg of catalyst. The reaction conditions were as follows: 500 ppm NO, 500 ppm NH_3, 5 vol.% O_2, and balance N_2 for the standard SCR reaction with a NO/NO_2 ratio of 1 : 0, and 500 ppm NO_x with NO/NO_2 ratios y (y = 4 : 1, 3 : 2, 1 : 1, 2 : 3, 1 : 4), 500 ppm NH_3, 5 vol.% O_2, and balance N_2 for the fast SCR reaction with different NO/NO_2 ratios. The NO_2-SCR reaction was tested in 500 ppm NO_2, 500 ppm NH_3, 5 vol.% O_2, and balance N_2. The total flow rate was 500 ml min^{-1}, and the effluent gas, including NO, NH_3, NO_2, and N_2O, was quantitatively detected by an online NEXUS 670-FTIR spectrometer. The spectra were collected at the steady state, and the NO_x conversion and N_2 selectivity were calculated according to the equations:

$$\mathrm{NO}_x\ \text{conversion} = \left(1 - \frac{[\mathrm{NO}]_{out} + [\mathrm{NO_2}]_{out}}{[\mathrm{NO}]_{in} + [\mathrm{NO_2}]_{in}}\right) \times 100\% \quad (1)$$

$$\mathrm{N_2}\ \text{selectivity} = \frac{[\mathrm{NO}]_{in} + [\mathrm{NH_3}]_{in} - [\mathrm{NO_2}]_{out} - 2[\mathrm{N_2O}]_{out}}{[\mathrm{NO}]_{in} + [\mathrm{NH_3}]_{in}} \times 100\% \quad (2)$$

2.2 Characterization

The *in situ* DRIFTS experiments were conducted using an FTIR spectrometer (Nicolet Nexus 670) with an MCT/A detector cooled with liquid nitrogen and a smart collector. The experimental temperature was precisely controlled by an Omega programmable temperature controller. Before each adsorption experiment, the catalyst was first pretreated at 400 °C for 0.5 h in a flow of 20 vol.% O_2/N_2 and then cooled down to comparatively low temperature (150 °C). The DRIFTS experiments of the fast SCR and standard SCR reactions were performed at 150 °C. The background spectrum was collected in flowing N_2 and was subtracted from the sample spectrum automatically. Both the adsorption and the reaction experiments were tested with a total flow rate of 300 ml min^{-1}. The adsorption conditions were controlled as follows: 500 ppm NH_3 or 500 ppm NO or 500 ppm NO_2, and N_2 balance for adsorption experiments. The reaction conditions were: 500 ppm NO, 500 ppm NH_3, 5 vol.% O_2, and balance N_2 for the standard SCR reaction, and 500 ppm NO_x with a NO/NO_2 ratio of 1 : 1, 500 ppm NH_3, 5 vol.% O_2, and balance N_2 for the fast SCR reaction. All DRIFTS spectra were recorded by accumulating 100 scans with a resolution of 4 cm^{-1}.

3. Results

3.1 NH_3-SCR activity

To gain a deep insight into the effect of the NO/NO_2 ratio on the NH_3-SCR activity, a systematic study was conducted by varying the NO/NO_2 ratio over a range spanning from 1 : 0 to 0 : 1 in the feed gas. Fig. 1 illustrates the NO conversion and N_2 selectivity as a function of reaction temperature under different gas compositions with NO/NO_2 ratios of 1 : 0, 4 : 1, 3 : 2, 1 : 1, 2 : 3, 1 : 4, and 0 : 1 over $CeWO_x$. As shown in Fig. 1(a) and (b), the $CeWO_x$ catalyst showed more than

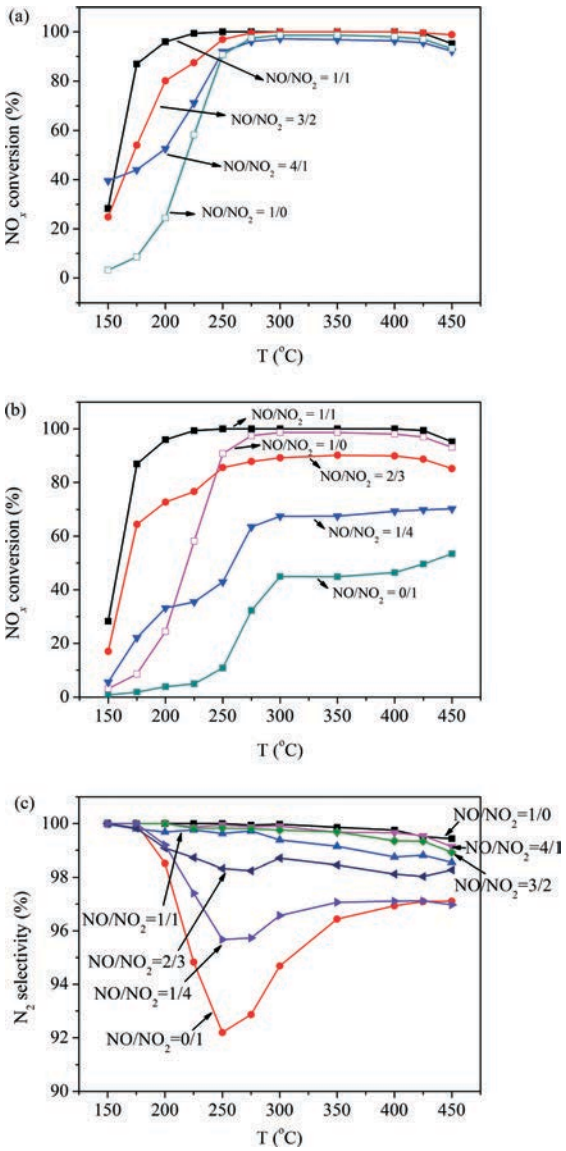

Fig. 1 NO_x conversion and N_2 selectivity over $CeWO_x$.

90% NO_x conversion from 250 to 450 °C under a GHSV of ~600 000 h^{-1} in the absence of NO_2, and the NO_x conversion was less than 60% below 250 °C. It should be noted that the NO_x conversion increased significantly with increasing NO_2 content until the NO/NO_2 ratio was 1 : 1 at low temperatures (≤200 °C), as shown in Fig. 1(a). Both the highest low temperature NO_x conversion and the widest operation temperature window were obtained when the NO/NO_2 ratio was 1 : 1. As seen in Fig. 1(b), further increase of the NO_2 concentration to an NO/NO_2 ratio of 1 : 4 decreased the NO_x conversion dramatically below 200 °C. However, in comparison with standard SCR, the NO_x conversion was higher at low temperatures (≤200 °C) as long as both NO_2 and NO were present in the feed. The activity results on the $CeWO_x$ catalyst clearly showed that the presence of NO_2 indeed promoted greatly the low temperature NO_x elimination, and this promotional effect was closely related to the NO_2 concentration in the feed gas. Similar conclusions have also been drawn for zeolite and V-based oxides.[35–38] However, when the NO/NO_2 ratio was 0 : 1 (NO_2-SCR), the NO_x conversion was below 60% over the whole temperature range, indicating that both NO and NO_2 in the feed were necessary for obtaining high NO_x conversion.

As seen in Fig. 1(c), N_2 selectivity was higher than 98% when the NO/NO_2 ratio was higher than 1/1, and the increase in NO_2 concentration decreased the N_2 selectivity slightly to 92%, due to the facilitation of N_2O formation by the reaction between NO_2 and NH_3.[36] It has to be pointed out that the NO/NO_2 ratio had a negligible effect on N_2 selectivity below 200 °C, therefore, the present study focused on the effect of NO/NO_2 ratio on NO_x conversion instead of N_2 selectivity.

3.2 *In situ* DRIFTS studies

3.2.1 NO adsorption on pre-adsorbed NO_2. In order to confirm whether NO could interact with the adsorbed NO_2 species, an *in situ* DRIFTS study was performed on the NO_2-pretreated $CeWO_x$ catalyst at 150 °C. The catalyst was first purged with NO_2 until saturation, followed by N_2 purging to remove the physisorbed NO_2 molecules. Then NO/N_2 was introduced, and the spectra were recorded as a function of time. The resulting spectra are shown in Fig. 2(a), and the simultaneous detection results of the effluent gases by an

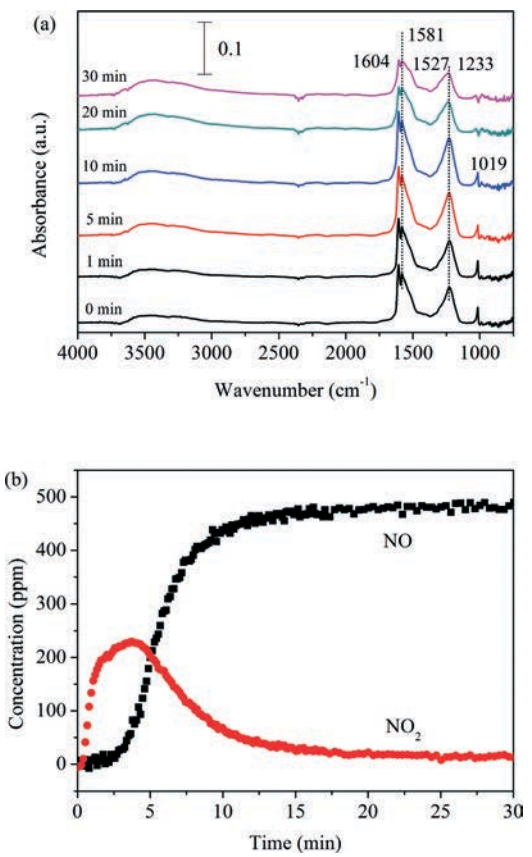

Fig. 2 *In situ* DRIFTS results of $CeWO_x$ treated in flowing 500 ppm NO_2 in N_2 until saturation and then purged with 500 ppm NO in N_2 at 150 °C (a), and the results of detecting the effluent gases (b).

online NEXUS 670-FTIR spectrometer are shown in Fig. 2(b). After NO_2 adsorption, bands at 1019, 1233, 1527, 1581, and 1604 cm^{-1} were observed. The bands at 1019 and 1581 cm^{-1} could be ascribed to bidentate nitrate,[18] whereas the bands at 1233 and 1604 cm^{-1} could be ascribed to bridging nitrate, and 1527 cm^{-1} was assigned to monodentate nitrate.[20] After NO was introduced into the cell, the wavenumbers of the nitrate species did not change, while all peak intensities of nitrate species decreased. As seen in Fig. 2(b), NO_2 produced by the reaction between NO and the surface oxygen atoms or the reaction between NO and the surface nitrates, evolved simultaneously. The decrease in the peak intensities within 10 min was insignificant, which could be ascribed to the effect of the surface nitrates formed by NO adsorption. These results indicated that NO could react with the surface nitrate species to form NO_2. Similar results have been obtained for Fe-ZSM-5 during fast SCR.[30]

3.2.2 NO_2 adsorption on pre-adsorbed NO. The DRIFTS results of NO_2 adsorption on pre-adsorbed NO were also obtained so as to make a comparison with the results of NO adsorption on pre-adsorbed NO_2. As shown in Fig. 3(a), after NO adsorption, bands at 1019, 1230, 1527, 1581, and 1604 cm^{-1} were observed, and the wavenumbers of the bands were almost identical to those after NO_2 adsorption, suggesting that NO could react with surface oxygen to form surface nitrates. On the other hand, the peaks of the nitrate species increased dramatically after the successive adsorption of NO_2, indicating that more nitrate species formed on the $CeWO_x$ surface. However, the successive treatment of NO and O_2 after NO adsorption did not increase the amount of surface nitrates, as shown in Fig. 3(b), indicating that no oxygen vacancies were present on the surface after the pretreatment of $CeWO_x$ by O_2 at 400 °C. These results also showed that the oxidation of NO by O_2 at 150 °C could not produce enough NO_2 to adsorb the surface nitrates on the surface of $CeWO_x$, indicating that the NO_2 formation by NO oxidation was slow over the $CeWO_x$ catalyst. Therefore, the amount of surface nitrate species formed by NO_2 was much greater than that by NO alone or the mixture of NO and O_2.

3.2.3 NO_2 adsorption on pre-adsorbed NH_3. To confirm if the adsorbed NH_3 could react with NO_2, the catalyst was first treated with NH_3 until saturation and purged with N_2. NO_2 was then introduced into the cell for 30 min, and the spectra recorded at different time intervals are shown in Fig. 4. After NH_3 adsorption, bands at 1181, 1256, 1423, 1590, 1671, and 3000–3400 cm^{-1} were observed. The bands at 1671 and 1423 cm^{-1} could be ascribed to the Brønsted ammonia

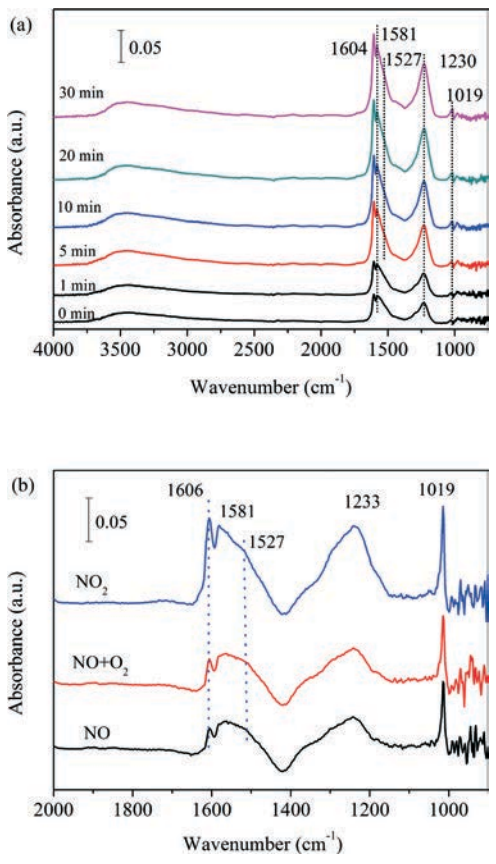

Fig. 3 (a) *In situ* DRIFTS results of $CeWO_x$ treated in flowing 500 ppm NO in N_2 until saturation, and then purged with 500 ppm NO_2 in N_2 successively at 150 °C. (b) *In situ* DRIFTS results of $CeWO_x$ treated in flowing 500 ppm NO in N_2 until saturation, and then purged with 500 ppm NO + 5% O_2 and 500 ppm NO_2 in N_2 successively at 150 °C.

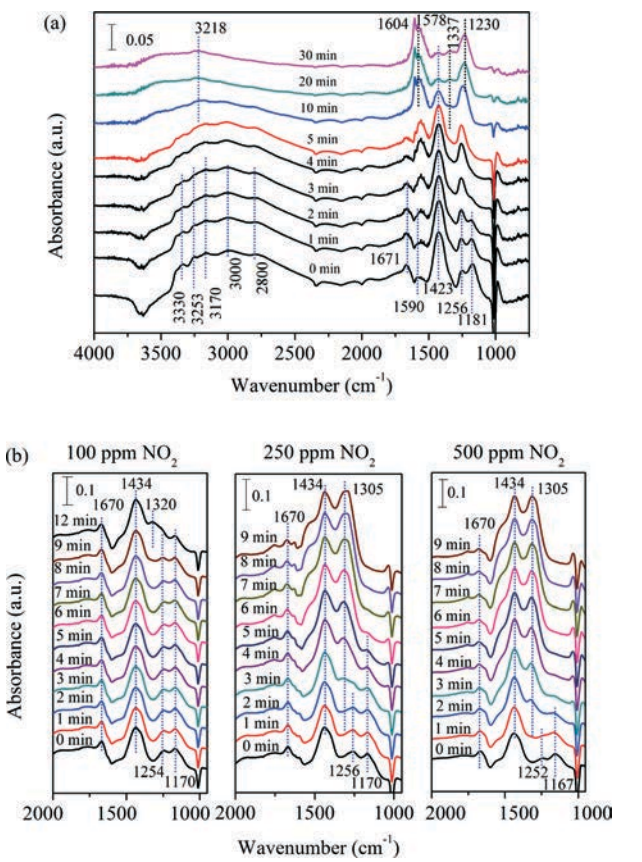

Fig. 4 *In situ* DRIFTS results of NH_3-presorbed $CeWO_x$ treated by flowing 500 ppm NO_2 in N_2 at 150 °C (a), and by flowing 100, 250, and 500 ppm NO_2 at room temperature (b).

species (NH_4^+-B),[20] whereas the bands at 1590, 1256, and 1181 cm^{-1} could be ascribed to Lewis ammonia species (NH_3-L).[15,16,18,20] After NO_2 was introduced into the cell, the band of NH_3-L species at 1181 cm^{-1} disappeared completely within 3 min, and the peaks of NH_4^+-B species decreased gradually with time on stream. The bands of the nitrate species at 1604, 1578, and 1230 cm^{-1} increased, indicating that NO_2 reacted with both the surface NH_3-L and NH_4^+-B species. These results were consistent with what was reported in the literature[21] by Chen *et al.* that both the Lewis and the Brønsted ammonia species on the Ce–W catalyst could participate in the NH_3-SCR reaction. It has to be noted that new bands at 1337 and ~3218 cm^{-1} were formed after NO_2 was introduced. Nova *et al.*[31] found that the DRIFTS result of pure NH_4NO_3 presented bands at 1380 and 3150 cm^{-1},which was quite similar to our results. In addition, Liu *et al.*[39] conducted a Fourier transform infrared spectroscopy study on NH_4NO_3 and found a peak at 1338 cm^{-1} that was ascribed to NO_3^-, and this wavenumber was the same as that reported in the present study. Therefore, the band at 1337 cm^{-1} could be ascribed to NH_4NO_3.

In order to investigate the correlation between the NO_2 concentration and the NH_4NO_3 formation, different amounts of NO_2 were introduced onto the surface of the NH_3-preadsorbed $CeWO_x$ catalyst. The experiment was performed at room temperature since the peak of NH_4NO_3 was weak which would easily be interfered by the other peaks (see Fig. 4(a)). As seen in Fig. 4(b), introducing 100 ppm NO_2 produced a new band at 1320 cm^{-1}, whereas increasing the NO_2 concentration to 250 ppm or more produced a band at 1305 cm^{-1}. The formation of these new bands was accompanied by the slight consumption of the adsorbed NH_3. Therefore, the bands at 1320 and 1305 cm^{-1} were also proposed to be NH_4NO_3.

To confirm the conclusions above, an *in situ* DRIFTS study of the $CeWO_x$ catalyst pre-impregnated by NH_4NO_3 (57 μmol g_{cat}^{-1}) or pretreated by NO_2 and NH_3 at room temperature was conducted. As shown in Fig. 5(a), the bands at 1030, 1305, and 1765 cm^{-1} could be ascribed to the nitrates in NH_4NO_3, whereas the bands at 1440, 2810, 3022, and 3200 cm^{-1} could be assigned to the NH_4^+ species in NH_4NO_3.[39] Consequently, the bands at 1305 and 3200 cm^{-1} could be assigned to NH_4NO_3 on the surface. Additionally, the subsequent adsorption of NH_3 on the NO_2-presorbed $CeWO_x$ catalyst at room temperature was also investigated in the present study, as shown in Fig. 5(b). Besides the adsorbed NH_4^+-B and NH_3-L, bands at 1323 and ~3200 cm^{-1} were also observed, indicating that NH_4NO_3 could be formed on $CeWO_x$ by the reaction between ammonia and surface nitrates. It has to be pointed out that a shift in the NH_4NO_3 band was observed from 1337 (Fig. 4(a)) to 1320/1323 (Fig. 4(b) and 5(b)) and 1305 cm^{-1} (Fig. 4(b) and 5(a)), which might be due to the differences in coverage or different phases[40] of NH_4NO_3 caused by the different formation procedures. Therefore, it was reasonable to suggest that the bands at 1337, 1320, 1305, and ~3218 cm^{-1} in Fig. 4 were representatives of the NH_4NO_3 intermediate on the surface of the $CeWO_x$ catalyst. The results in Fig. 4 and 5 indicate that the surface ammonia species might react with NO_2 gas according to the following equation:

$$2NH_3 + 2NO_2 \leftrightarrow NH_4NO_3 + N_2 + H_2O \quad (3)$$

This reaction has been reported by Grossale *et al.*[41,42] to take place below 250 °C on Fe/zeolite catalysts. It has been reported that reaction (3) was a result of the combination of the following steps:[41]

$$2NO_2 + H_2O \leftrightarrow HNO_3 + HONO \quad (4)$$

$$NH_3 + HONO \rightarrow [NH_4NO_2] \rightarrow N_2 + 2H_2O \quad (5)$$

$$NH_3 + HNO_3 \leftrightarrow NH_4NO_3 \quad (6)$$

These reactions might also take place in the reaction between NO_2 and NH_3 on $CeWO_x$.

As seen in Fig. 4(b), NH_4NO_3 was produced within 3 min when the NO_2 concentration was 500 ppm, whereas decreasing the concentration of NO_2 to 250 ppm led to the formation of NH_4NO_3 after 3 min. It has to be noted that no peak of NH_4NO_3 could be observed within 10 min when the NO_2 concentration was further decreased to 100 ppm, indicating that the lower NO_2 concentration resulted in the smaller amount of NH_4NO_3 within the same time period.

3.2.4 The decomposition of NH_4NO_3 at 150 °C. To study the stability of NH_4NO_3 at low temperature, an *in situ* DRIFTS study was also conducted over the NH_4NO_3-impregnated $CeWO_x$ catalyst at 150 °C. As shown in Fig. 5c, the band at 1271 cm^{-1} could be assigned to the contribution of both NH_3-L (at 1256 cm^{-1}) and NH_4NO_3 (at 1305 cm^{-1}), and the new bands at 1513 and 1673 cm^{-1} at 150 °C could be ascribed to the surface monodentate nitrate and NH_4^+-B, indicating that the adsorbed ammonia and nitrates appeared simultaneously on the surface of the NH_4NO_3-impregnated

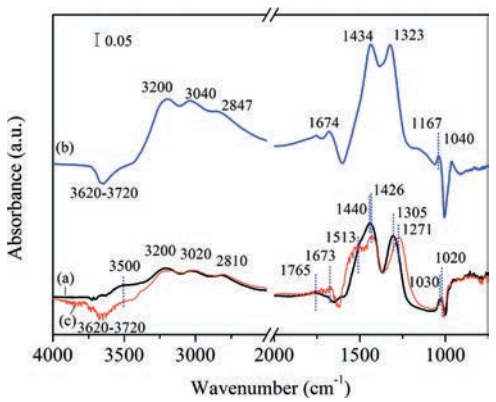

Fig. 5 *In situ* DRIFTS results of $CeWO_x$ pre-impregnated with NH_4NO_3 at room temperature (a) and at 150 °C (c), and $CeWO_x$ treated with 500 ppm NO_2 in N_2 until saturation, and with 500 ppm NH_3 in N_2 successively for 30 min at room temperature (b).

catalyst at 150 °C. In addition to the changes above, the simultaneous slight decrease in the band at 3200 cm^{-1} demonstrated that NH_4NO_3 decomposed to surface nitrates and ammonia following the equation:

$$NH_4NO_3 \leftrightarrow NH_3 + HNO_3$$

This is the reverse reaction of reaction (6). It is widely accepted that NH_4NO_3 is solid below 170 °C and could decompose to NH_3 and HNO_3 in the melt above 170 °C.[33] However, Koebel *et al.*[43] found that ammonium nitrate deposited on a monolith catalyst at 150 °C decomposed to NH_3 and HNO_3 soon after the temperature started to rise, due to the presence of H_2O in the feed. Similarly, Madany and Burnet[44] pointed out in their paper that the presence of H_2O could promote the reverse reaction of eqn (6). Although the NH_4NO_3-impregnated $CeWO_x$ catalyst had been dried in air overnight and purged with N_2 for 1 h at room temperature before collecting the spectra, adsorbed H_2O might still have remained on the surface of the catalyst. Therefore, it is possible that a small part of NH_4NO_3 decomposed to NH_3 and HNO_3 at 150 °C in the present study.

In order to make clear whether the surface NH_4NO_3 participates in the NH_3-SCR reaction, *in situ* DRIFTS studies were conducted on the decomposition of NH_4NO_3 both in N_2 and in NO/N_2. The peaks of NH_4NO_3 had no obvious change with the time on stream in N_2, as shown in Fig. 6(a), indicating that the decomposition of NH_4NO_3 in N_2 is a slow process at 150 °C. Nevertheless, the treatment of the NH_4NO_3-impregnated $CeWO_x$ catalyst in NO/N_2 resulted in a dramatic reduction of the peaks of NH_4NO_3 at 1271, 1426, 2810, 3020, 3180, and 3250 cm^{-1} within 30 min, as shown in Fig. 6(b). The reduction of the band at 1271 cm^{-1} to the bands of 1305 and 1256 cm^{-1} proved that the peak at 1271 cm^{-1} was indeed the contribution of both NH_4NO_3 and NH_3-L. Compared with Fig. 6(a), the consumption of NH_4NO_3 was much faster in NO/N_2 than in N_2, indicating that NO in the gas phase could react with NH_4NO_3. To investigate the products of the NH_4NO_3 reduction by NO, the effluent gases were simultaneously analyzed by an online NEXUS 670-FTIR spectrometer. NO_2 was evolved accompanied by the reduction of NH_4NO_3 by NO, as shown in Fig. 6(c). The facilitation of NH_4NO_3 decomposition by NO was suggested to proceed according to the following equation over many catalysts, *e.g.*, V_2O_5–WO_3/TiO_2 (ref. 31) and Fe/ZSM-5.[41]

$$NH_4NO_3 + NO \rightarrow N_2 + NO_2 + 2H_2O \quad (7)$$

3.2.5 Co-adsorption of NO_2 and NO on pre-adsorbed NH_3. In order to study the effect of NO on the reaction between the adsorbed NH_3 and NO_2 gas, the following experiment was conducted. Similar to the experimental procedure for the study of NO_2 adsorption on pre-adsorbed NH_3, the catalyst was first treated with NH_3 until saturation and then purged with N_2. Afterwards, the mixture of NO_2 and NO was introduced for 30 min. The spectra are shown in Fig. 7. After the

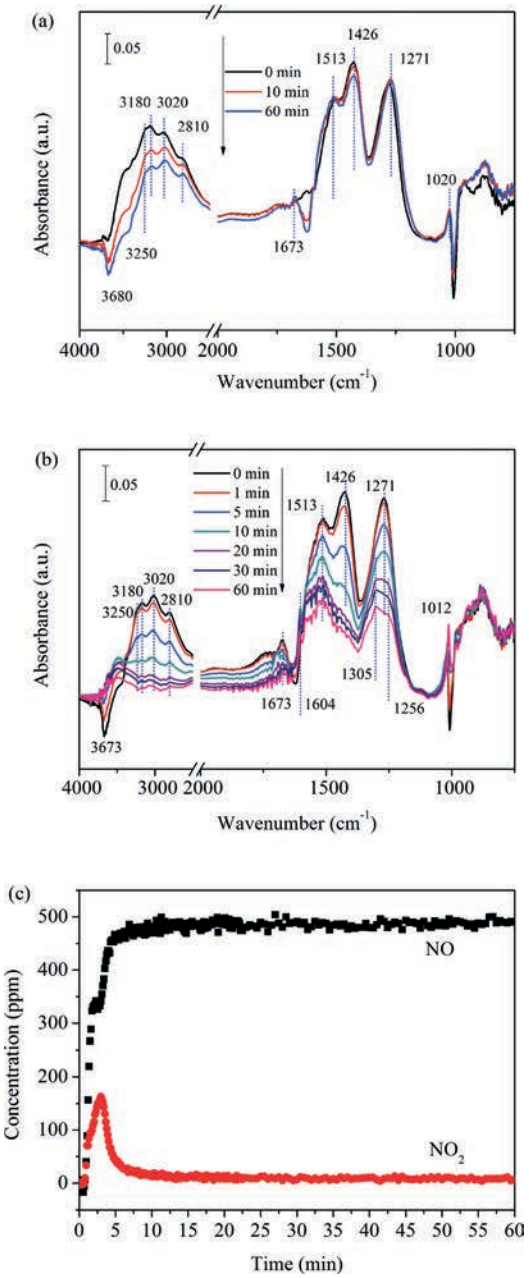

Fig. 6 *In situ* DRIFTS results of NH_4NO_3-impregnated $CeWO_x$ treated in N_2 (a) at 150 °C and by flowing 500 ppm NO in N_2 (b) at 150 °C. (c) The concentration of NO and NO_2 in the effluent gases during the experiment (b) analyzed by an online NEXUS 670-FTIR spectrometer.

mixture of NO_2 and NO was introduced into the cell, all the adsorbed ammonia species decreased quickly with time on stream, and disappeared completely after 2 min, leaving only the bands of nitrate species at 1604, 1581, 1230, and 1020 cm^{-1} in the spectra. Compared with Fig. 4(a), it can be observed that the mixture of NO_2 and NO reacted faster with the surface NH_3 and NH_4^+ species than NO_2 alone. These results were consistent with the activity result that fast SCR in the presence of NO_2 showed better performance than NO_2-SCR (NO/NO_2 = 0 : 1). Additionally, no bands at 1337 and ~3218 cm^{-1} were observed in the presence of NO, indicating

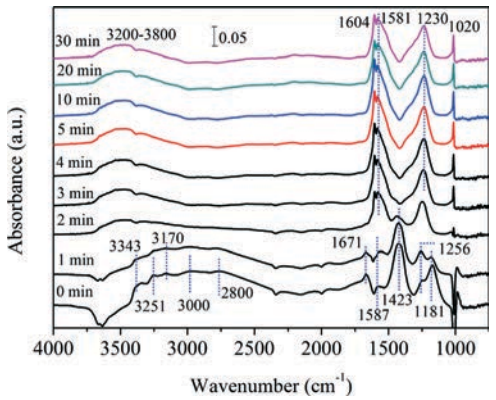

Fig. 7 *In situ* DRIFTS results of NH_3-presorbed $CeWO_x$ treated by flowing 250 ppm NO_2 + 250 ppm NO in N_2 at 150 °C.

that the presence of NO might accelerate the decomposition of NH_4NO_3 species, although it was not easy for the NH_4NO_3 intermediate on the surface of the catalyst to decompose to NH_3 and HNO_3 below 170 °C.[33] Another reasonable explanation for the absence of NH_4NO_3 was that the reduction of the surface nitrates by NO is faster than the formation of NH_4NO_3.

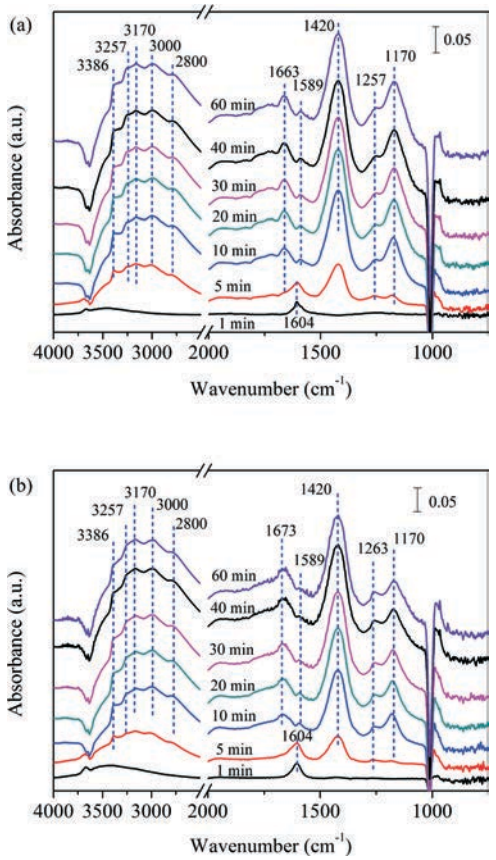

Fig. 8 *In situ* DRIFTS results of $CeWO_x$ after the standard SCR reaction (a) and the fast SCR reaction (b) at 150 °C. The NO/NO_2 ratio was 1 : 1 for the fast SCR reaction.

3.2.6 Fast SCR and standard SCR. To identify the species present on $CeWO_x$ catalysts during fast SCR and standard SCR, an *in situ* DRIFTS study was conducted at 150 °C. As seen in Fig. 8, bridging nitrate (the band at 1604 cm^{-1}) was formed after the introduction of the reactant gas for 1 min, and then the bridging nitrate peak decreased with time on stream after 5 min accompanied by the increase in the adsorbed NH_3 species, indicating that the surface nitrates formed by NO or NO_2 could participate in the NH_3-SCR reaction.[20] Under steady state conditions, NH_3-L and NH_4^+-B were present on the surface of the $CeWO_x$ catalyst during both standard and fast SCR. It should be noted that no NH_4NO_3 was observed during either standard or fast SCR, indicating that either NH_4NO_3 decomposed rapidly, or was not formed from the beginning due to the faster reaction between NO and the surface nitrates. However, the results in the present study show that if reaction (7) took place, the reaction between NO and NH_4NO_3 during standard SCR and fast SCR was extremely fast.

4. Discussion

4.1 Formation of surface nitrates and nitrite

Based on previous reports, CeO_2 was suggested to be the main active site for the NH_3-SCR reaction.[12,20,21] It can be suggested that NO activation on the $CeWO_x$ catalyst follows the equations:[23]

$$NO + [Ce^{4+}]\text{–}O \leftrightarrow [Ce^{4+}]\text{–}ONO(\text{nitrite}) \quad (8)$$

$$2[Ce^{4+}]\text{–}O + NO \rightarrow [2Ce^{4+}]{=}O_2NO\ (\text{bridging nitrate}) \quad (9)$$

$$O\text{–}[Ce^{4+}]\text{–}O + NO \rightarrow [Ce^{4+}]{=}O_2NO\ (\text{bidentate nitrate}) \quad (10)$$

and the adsorption of NO_2 on the catalyst follows the equation:

$$[Ce^{4+}]\text{–}O + NO_2 \rightarrow [Ce^{4+}]\text{–}ONO_2(\text{monodentate nitrate}) \quad (11)$$

It is clear that NO_2 can be adsorbed on one $[Ce^{4+}]$–O site to form one monodentate nitrate ($[Ce^{4+}]$–ONO_2), whereas the adsorption of NO needs two $[Ce^{4+}]$–O sites to produce one bidentate nitrate ($[Ce^{4+}]{=}O_2NO$) or one bridging nitrate ($[2Ce^{4+}]{=}O_2NO$). In addition, the presence of NO could reduce the amount of surface nitrates, as shown in Fig. 2. Since no surface nitrite species ($[Ce^{4+}]$–ONO) was observed in the present study, it can be concluded that the surface nitrite species was extremely active and was desorbed too fast to be detected by DRIFTS. Therefore, NO gas reacted with the surface nitrates to form NO_2 gas according to the equations:[41]

$$[Ce^{4+}]\text{–}ONO_2(\text{monodentate nitrate}) + NO \leftrightarrow [Ce^{4+}]\text{–}ONO + NO_2 \quad (12)$$

$$[2Ce^{4+}]{=}O_2NO\ (\text{bridging nitrate}) + NO \leftrightarrow [Ce^{4+}]\text{–}ONO + NO_2 + [Ce^{3+}]\text{–}\square \quad (13)$$

$$[Ce^{4+}]{=}O_2NO \text{ (bidentate nitrate)} + NO \leftrightarrow [Ce^{4+}]\text{–}ONO + NO_2 \quad (14)$$

$$[Ce^{4+}]\text{–}ONO \leftrightarrow [Ce^{3+}]\text{–}\square + NO_2 \quad (15)$$

The mutual transformation between the monodentate, bridging and bidentate nitrate follows the equations:[45,46]

$$[2Ce^{4+}]{=}ONO_2\text{(bridging nitrate)} \leftrightarrow [Ce^{4+}]\text{–}ONO_2\text{(monodentate nitrate)} + [Ce^{3+}]\text{–}\square \quad (16)$$

$$[Ce^{4+}]{=}O_2NO \text{ (bidentate nitrate)} \leftrightarrow [Ce^{4+}]\text{–}ONO_2\text{(monodentate nitrate)} \quad (17)$$

These transformations made it possible for the monodentate, bridging and bidentate nitrate species to all be present on the surface of the $CeWO_x$ catalyst after the adsorption of NO or NO_2.

After the surface was saturated with the nitrates originating from NO adsorption, NO_2 could still be adsorbed on the surface according to the equation:[41]

$$[Ce^{3+}]\text{–}\square + 2NO_2 \leftrightarrow [Ce^{4+}]\text{–}ONO_2\text{(monodentate nitrate)} + NO \quad (18)$$

This equation is a combination of the reverse reaction of eqn (12) and (15). The presence of NO_2 could reoxidize the low valence Ce species,[28] and the saturated adsorption of NO cannot inhibit the adsorption of NO_2.

4.2 Mechanism of SCR reactions

Many researchers reported that NH_4NO_3 is reducible by NO above its melting point of 170 °C,[32,47] and in the melt, NH_4NO_3 can decompose to NH_3 and HNO_3. NO could reduce HNO_3 to HNO_2 at a comparatively lower temperature, *i.e.* at 50 °C.[41] However, it is obvious that NO was able to reduce NH_4NO_3 significantly at 150 °C in the present study, and this reaction rate was faster than that of NH_4NO_3 decomposition to NH_3 and HNO_3 in N_2, as shown in Fig. 6. Therefore, it could be suggested that NO gas reduced NH_4NO_3 directly according to eqn (7), rather than reacting with the nitrates formed by the decomposition of NH_4NO_3. It is widely accepted that the formation of NH_4NO_3 blocks the active site of the NH_3-SCR reaction,[42,48,49] and eqn (7) has been suggested to be crucial in the NH_3-SCR reaction by many researchers, since it consumes NH_4NO_3 on the surface of the catalysts.[32,41,50] Koebel *et al.*[43] suggested that eqn (7) was more important at lower temperature, and this reaction governed the whole NO_x conversion at 140 °C over the V_2O_5–WO_3/TiO_2 catalyst. Wang *et al.*[50] observed the presence of NH_4NO_3 during the fast SCR reaction instead of the standard SCR reaction over the Cu-SAPO-34 catalyst, and suggested that the reaction between NO and NH_4NO_3 was important for fast SCR. Iwasaki and Shinjoh[51] reported that eqn (7) was the rate-limiting step for the fast SCR reaction over the Fe-ZSM-5 catalyst. A similar conclusion has been drawn by Grossale *et al.*[42] In the present study, no NH_4NO_3 was present on the surface of the $CeWO_x$ catalyst under standard and fast SCR reaction conditions at 150 °C, as seen in Fig. 8, indicating that if reaction (7) occurred, it must be very fast. This might be the reason why $CeWO_x$ performed excellently during both standard and fast SCR.

Nevertheless, NO could still react with the surface nitrate species according to eqn (12)–(14). In this case, NH_4NO_3 could not be formed due to the faster reaction between the surface nitrates and NO. As shown by eqn (12)–(14), NO could react with the surface nitrates to produce NO_2 gas and nitrite intermediates. These nitrites, which might be too active to be observed during DRIFT studies, will either desorb from the surface of the catalyst to produce NO_2 gas, or react with the adsorbed ammonia to form N_2 in the SCR reaction. The importance of eqn (12)–(14) in the NH_3-SCR reaction has been reported by many groups. Nova *et al.*[31] found that NO could react with nitric acid at 200 °C on the commercial V_2O_5–WO_3/TiO_2 catalyst, forming NO_2 and nitrous acid (HONO), and the fast SCR reaction is limited by this reaction at low temperatures. Additionally, Ruggeri *et al.*[30] suggested that the reduction of nitrates/nitric acid by NO was a crucial step in the fast SCR reaction over Fe/ZSM-5 based on the results of a DRIFTS study. Grossale *et al.*[35] proposed that the surface nitrates were the key intermediates for oxidizing NO during fast SCR, which could be reduced by ammonia during the NO_2-SCR reaction over Cu- or Fe- zeolites. The present results are consistent with those reported in the literature for V-based oxides and zeolite catalysts. Therefore, it could be proposed that eqn (12)–(14) are important, and both the surface nitrate and NO in the gas phase are necessary for the formation of active nitrites.

The SCR reaction might proceed according to the following equations at low temperatures (≤200 °C):

1. The formation of surface nitrites from NO or NO_2 adsorption:

$$NO + [Ce^{4+}]\text{–}O \leftrightarrow [Ce^{4+}]\text{–}ONO \quad (8)$$

$$NO_2 + [Ce^{3+}]\text{–}\square \leftrightarrow [Ce^{4+}]\text{–}ONO \quad (15)$$

2. The formation of surface nitrates from NO or NO_2 adsorption:

$$2[Ce^{4+}]\text{–}O + NO \rightarrow [2Ce^{4+}]ONO_2 \quad (9)$$

$$O\text{–}[Ce^{4+}]\text{–}O + NO \rightarrow [Ce^{4+}]{=}O_2NO \quad (10)$$

$$[Ce^{4+}]\text{–}O + NO_2 \rightarrow [Ce^{4+}]\text{–}ONO_2 \quad (11)$$

3. Reactions between NO and surface nitrates:

$$[Ce^{4+}]\text{–}ONO_2 + NO \leftrightarrow [Ce^{4+}]\text{–}ONO + NO_2 \quad (12)$$

$$[2Ce^{4+}]{=}O_2NO + NO \leftrightarrow [Ce^{4+}]\text{–}ONO + NO_2 + [Ce^{3+}]\text{–}\square \quad (13)$$

$$[Ce^{4+}]{=}O_2NO + NO \leftrightarrow [Ce^{4+}]\text{–}ONO + NO_2 \quad (14)$$

4. Reactions between surface nitrites and adsorbed ammonia:

$$[Ce^{4+}]\text{–}ONO + NH_3\text{–}L \rightarrow [Ce^{4+}]\text{–}OH + NH_2NO \rightarrow N_2 + H_2O + [Ce^{4+}]\text{–}OH \quad (19)$$

$$[Ce^{4+}]\text{–}ONO + NH_4^+\text{–}B \rightarrow [Ce^{3+}]\text{–}\square + NH_4NO_2 \rightarrow N_2 + 2H_2O + [Ce^{3+}]\text{–}\square \quad (20)$$

5. Reaction between surface NH_4NO_3 and NO gas:

$$NH_4NO_3 + NO \rightarrow N_2 + NO_2 + 2H_2O \quad (7)$$

For standard SCR, the surface nitrates originated mainly from direct NO adsorption on the surface, or from the adsorption of NO_2 produced by NO oxidation. Therefore, the amount of NO_2 produced during NO oxidation over $CeWO_x$ was determined. As seen in Fig. 9, the amount of NO_2 produced below 200 °C was less than 10 ppm, indicating that the reaction of NO oxidation to NO_2 was slow, which was consistent with the results shown in Fig. 3(b). Therefore, the surface nitrates mainly came from the adsorption of NO on the surface of the catalyst according to eqn (9) and (10). Since NO_2 adsorption led to the formation of more surface nitrates than NO adsorption, as seen in Fig. 3, NO tended to play the role of reducing NH_4NO_3 or nitrates. Consequently, it could be suggested that there was a close correlation between NO_x conversion and the amount of surface nitrates. The surface nitrates, mainly originating from NO_2, were essential intermediates for forming NH_4NO_3 or surface nitrites. The NO_x conversion depended on the concentration of NO_2 in the reactant gas,[36,37] as shown in Fig. 1. For NO_2-SCR, the concentration of surface nitrates and NH_4NO_3 must be the highest (see Fig. 4(b)). However, the lack of NO resulted in the accumulation of NH_4NO_3, which would block the surface active sites for activating NH_3 or NO_2,[49,50] resulting in the lowest NO_x conversion. Both NO and NO_2 were necessary for higher NO_x conversion, which confirmed that there was an optimized NO/NO_2 ratio of 1/1 for the SCR reaction when the overall amount of NO_x was fixed.

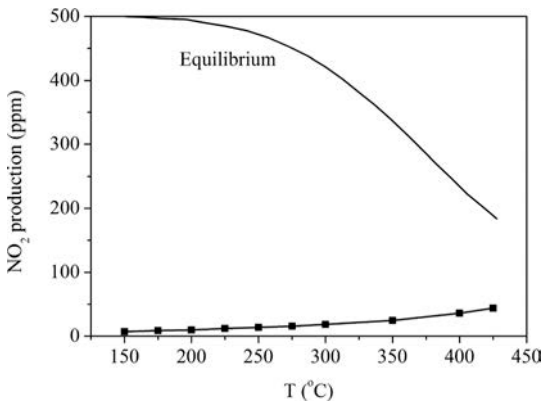

Fig. 9 NO_2 production during NO oxidation over $CeWO_x$. Reaction conditions: 500 ppm NO, 5 vol.% O_2, and N_2 balance.

5. Conclusions

The NO conversion on $CeWO_x$ catalysts followed the order of fast SCR > standard SCR > NO_2-SCR at low temperatures (<200 °C). An optimal NO/NO_2 feed ratio was suggested for the SCR reaction, and the best deNO_x efficiency was achieved at a NO/NO_2 feed ratio of 1 : 1. The DRIFTS study showed that the adsorption of NO or NO_2 resulted in the formation of the same surface nitrates, whereas NO_2 adsorption led to much more surface nitrates than NO adsorption. NO_2 is responsible for the formation of surface nitrates, which may further react with adsorbed NH_3 to form NH_4NO_3. NO participates in the reaction by following two pathways: one is to reduce NH_4NO_3 to form N_2 directly; the other is to reduce the surface nitrates to active nitrite species, which will react with the adsorbed NH_3 species to produce N_2. Both Lewis and Brønsted ammonia species on the $CeWO_x$ catalyst could participate in the fast SCR reaction. NH_4NO_3 was also observed during the reaction between NO_2 and NH_3, and it was suggested that NO could reduce NH_4NO_3 directly below its melting point.

In comparison with standard SCR, more surface nitrates were formed during the fast SCR reaction, leading to a higher NO_x conversion. For NO_2-SCR, although the amount of surface nitrates was higher, the lack of NO gas resulted in the blockage of the active sites by NH_4NO_3 on $CeWO_x$, and consequently, a lower NO_x conversion. The reactions between NO and NH_4NO_3 or surface nitrates at low temperatures were important for the NH_3-SCR reaction. Therefore, both NO in the gas phase and surface nitrates were important for the NH_3-SCR reaction.

Acknowledgements

This work was financially supported by the National Natural Science Foundation of China (51221892), China Postdoctoral Science Foundation (2012M520018) and the Ministry of Science and Technology of China (2013AA065301, 2010CB732304).

Notes and references

1 Z. M. Liu and S. I. Woo, *Catal. Rev.: Sci. Eng.*, 2006, **48**, 43–89.
2 P. Granger and V. I. Parvulescu, *Chem. Rev.*, 2011, **111**, 3155–3207.
3 T. V. Johnson, *Int. J. Engine Res.*, 2009, **10**, 275–285.
4 F. D. Liu, H. He and C. B. Zhang, *Chem. Commun.*, 2008, 2043–2045.
5 F. D. Liu, H. He, Y. Ding and C. B. Zhang, *Appl. Catal., B*, 2009, **93**, 194–204.
6 F. D. Liu, K. Asakura, H. He, Y. C. Liu, W. P. Shan, X. Y. Shi and C. B. Zhang, *Catal. Today*, 2011, **164**, 520–527.
7 Y. Li, H. Cheng, D. Y. Li, Y. S. Qin, Y. M. Xie and S. D. Wang, *Chem. Commun.*, 2008, 1470–1472.

8 Z. B. Wu, R. B. Jin, Y. Liu and H. Q. Wang, *Catal. Commun.*, 2008, **9**, 2217–2220.
9 B. X. Shen, T. Liu, N. Zhao, X. Y. Yang and L. D. Deng, *J. Environ. Sci.*, 2010, **22**, 1447–1454.
10 B. X. Shen, X. P. Zhang, H. Q. Ma, Y. Yao and T. Liu, *J. Environ. Sci.*, 2013, **25**, 791–800.
11 K. Cheng, J. Liu, T. Zhang, J. M. Li, Z. Zhao, Y. C. Wei, G. Y. Jiang and A. J. Duan, *J. Environ. Sci.*, 2014, **26**, 2106–2113.
12 W. Q. Xu, Y. B. Yu, C. B. Zhang and H. He, *Catal. Commun.*, 2008, **9**, 1453–1457.
13 Y. S. Shen, S. M. Zhu, T. Qiu and S. B. Shen, *Catal. Commun.*, 2009, **11**, 20–23.
14 X. Gao, Y. Jiang, Y. Fu, Y. Zhong, Z. Luo and K. Cen, *Catal. Commun.*, 2010, **11**, 465–469.
15 W. P. Shan, F. D. Liu, H. He, X. Y. Shi and C. B. Zhang, *ChemCatChem*, 2011, **3**, 1286–1289.
16 W. P. Shan, F. D. Liu, H. He, X. Y. Shi and C. B. Zhang, *Catal. Today*, 2012, **184**, 160–165.
17 L. Chen, J. H. Li, M. F. Ge and R. H. Zhu, *Catal. Today*, 2010, **153**, 77–83.
18 L. Chen, J. H. Li and M. F. Ge, *Environ. Sci. Technol.*, 2010, **44**, 9590–9596.
19 W. P. Shan, F. D. Liu, H. He, X. Y. Shi and C. B. Zhang, *Appl. Catal., B*, 2012, **115–116**, 100–106.
20 W. P. Shan, F. D. Liu, H. He, X. Y. Shi and C. B. Zhang, *Chem. Commun.*, 2011, **47**, 8046–8048.
21 L. Chen, J. H. Li, M. F. Ge, L. Ma and H. Z. Chang, *Cuihua Xuebao*, 2011, **32**, 836–841.
22 Z. R. Ma, D. Weng, X. D. Wu and Z. C. Si, *J. Environ. Sci.*, 2012, **24**, 1305–1316.
23 Y. Peng, K. Z. Li and J. H. Li, *Appl. Catal., B*, 2013, **140–141**, 483–492.
24 Z. M. Liu, S. X. Zhang, J. H. Li and L. L. Ma, *Appl. Catal., B*, 2014, **144**, 90–95.
25 F. D. Liu, H. He, C. B. Zhang, W. P. Shan and X. Y. Shi, *Catal. Today*, 2011, **175**, 18–25.
26 R. Q. Long and R. T. Yang, *J. Catal.*, 2001, **198**, 20–28.
27 G. Qi and R. T. Yang, *Appl. Catal., B*, 2003, **44**, 217–225.
28 M. Koebel, G. Madia, F. Raimondi and A. Wokaum, *J. Catal.*, 2002, **209**, 159–165.
29 Y. H. Yeom, J. Henao, M. J. Li, W. M. H. Sachtler and E. Weitz, *J. Catal.*, 2005, **231**, 181–193.
30 M. P. Ruggeri, A. Grossale, I. Nova, E. Tronconi, H. Jirglova and Z. Sobalik, *Catal. Today*, 2012, **184**, 107–114.
31 I. Nova, C. Ciardelli, E. Tronconi, D. Chatterjee and B. Bandl-Konrad, *Catal. Today*, 2006, **114**, 3–12.
32 C. Ciardelli, I. Nova, E. Tronconi, D. Chatterjee and B. Bandl-Konrad, *Chem. Commun.*, 2004, 2718–2719.
33 A. Savara, M. J. Li, W. M. H. Sachtler and E. Weitz, *Appl. Catal., B*, 2008, **81**, 251–257.
34 I. Nova, C. Ciardelli, E. Tronconi, D. Chatterjee and M. Weibel, *AIChE J.*, 2009, **55**, 1514–1529.
35 A. Grossale, I. Nova, E. Tronconi, D. Chatterjee and M. Weibel, *Top. Catal.*, 2009, **52**, 1837–1841.
36 M. Devadas, O. Kröcher, M. Elsener, A. Wokaun, N. Söger, M. Pfeifer, Y. Demel and L. Mussmann, *Appl. Catal., B*, 2006, **67**, 187–196.
37 I. Nova, C. Ciardelli, E. Tronconi, D. Chatterjee and M. Weibel, *Top. Catal.*, 2007, **42–43**, 43–46.
38 C. Ciardelli, I. Nova, E. Tronconi, D. Chatterjee, B. Bandl-Konrad, M. Weibel and B. Krutzsch, *Appl. Catal., B*, 2007, **70**, 80–90.
39 N. Liu, X. L. Wei, M. G. Gao, L. Xu, J. J. Tong, X. X. Li and L. Jin, *Guangpuxue Yu Guangpu Fenxi*, 2013, **33**, 1771–1774.
40 Z. X. Shen, M. H. Kuok and S. H. Tang, *Spectrochim. Acta*, 1993, **49**, 21–29.
41 A. Grossale, I. Nova and E. Tronconi, *J. Catal.*, 2009, **265**, 141–147.
42 A. Grossale, I. Nova, E. Tronconi, D. Chatterjee and M. Weibel, *J. Catal.*, 2008, **256**, 312–322.
43 M. Koebel, M. Elsener and G. Madia, *Ind. Eng. Chem. Res.*, 2001, **40**, 52–59.
44 G. H. Madany and G. Burnet, *J. Agric. Food Chem.*, 1968, **16**, 136–140.
45 B. Q. Jiang, Z. G. Li and S. C. Lee, *Chem. Eng. J.*, 2013, **225**, 52–58.
46 N. Tang, Y. Liu, H. Q. Wang and Z. B. Wu, *J. Phys. Chem. C*, 2011, **115**, 8214–8220.
47 M. Koebel, G. Madia and M. Elsener, *Catal. Today*, 2002, **73**, 239–247.
48 I. Malpartida, O. Marie, P. Bazin, M. Daturi and X. Jeandel, *Appl. Catal., B*, 2012, **113–114**, 52–60.
49 L. J. Xie, F. D. Liu, K. Liu, X. Y. Shi and H. Hong, *Catal. Sci. Technol.*, 2014, **4**, 1104–1110.
50 D. Wang, L. Zhang, K. Kamasamudram and W. S. Epling, *ACS Catal.*, 2013, **3**, 871–881.
51 M. Iwasaki and H. Shinjoh, *Appl. Catal., A*, 2010, **390**, 71–77.